Mol Cell Biochem (2016) 413:9–23
DOI 10.1007/s11010-015-2622-9

Vascular endothelial growth factor-C protects heart from ischemia/reperfusion injury by inhibiting cardiomyocyte apoptosis

Xu-guang Chen[1,3] · Yan-xia Lv[2] · Dan Zhao[2] · Lei Zhang[1] · Fei Zheng[1] · Jian-Ye Yang[1] · Xiao-lin Li[1] · Lu Wang[1] · Lin-Yun Guo[1] · Ya-mu Pan[1] · Yu-wen Yan[1] · Shi-You Chen[5] · Jia-Ning Wang[1,2] · Jun-Ming Tang[1,2] · Yu Wan[4]

Received: 14 July 2015 / Accepted: 8 December 2015 / Published online: 14 January 2016

Abstract VEGF-C is a newly identified proangiogenic protein playing an important role in vascular disease and angiogenesis. However, its role in myocardial ischemia/reperfusion (I/R) injury remains unknown. The objective of this study was to determine the role and mechanism of VEGF-C in myocardial ischemia–reperfusion injury. Rat left ventricle myocardium was injected with recombinant human VEGF-C protein (0.1 or 1.0 μg/kg b.w.) 1 h prior to myocardial ischemia–reperfusion (I/R) injury. 24 h later, the myocardial infarction size, the number of TUNEL-positive cardiomyocytes, the levels of creatine kinase (CK), CK-MB, cardiac troponin, malondialdehyde (MDA) content, and apoptosis protein Bax expression were decreased, while Bcl2 and pAkt expression were increased in VEGF-C-treated myocardium as compared to the saline-treated I/R hearts. VEGF-C also improved the function of I/R-injured hearts. In the H_2O_2-induced H9c2 cardiomyocytes, which mimicked the I/R injury in vivo, VEGF-C pre-treatment decreased the LDH release and MDA content, blocked H_2O_2-induced apoptosis by inhibiting the pro-apoptotic protein Bax expression and its translocation to the mitochondrial membrane, and consequently attenuated H_2O_2-induced decrease of mitochondrial membrane potential and increase of cytochrome c release from mitochondria. Mechanistically, VEGF-C activated Akt signaling pathway via VEGF receptor 2, leading to a blockade of Bax expression and mitochondrial membrane translocation and thus protected cardiomyocyte from H_2O_2-induced activation of intrinsic apoptotic pathway. VEGF-C exerts its cardiac protection following I/R injury via its anti-apoptotic effect.

Keywords Ischemia–reperfusion · Cardiomyocyte · VEGF-C · Apoptosis · H_2O_2

Xu-guang Chen and Yan-xia Lv are co-first authors.

Electronic supplementary material The online version of this article (doi:10.1007/s11010-015-2622-9) contains supplementary material, which is available to authorized users.

✉ Jun-Ming Tang
tangjm416@163.com

✉ Yu Wan
wanyu@whu.edu.cn

1 Institute of Clinical Medicine and Department of Cardiology, Renmin Hospital, Hubei University of Medicine, Shiyan, 442000 Hubei, China

2 Department of Physiology and Key Lab of Human Embryonic Stem Cell of Hubei Province, Hubei University of Medicine, Shiyan, 442000 Hubei, People's Republic of China

3 Department of Dermatology, Renmin Hospital, Hubei University of Medicine, Shiyan, 442000 Hubei, People's Republic of China

4 Center for Medical Research and Department of Physiology, School of Basic Medical Sciences, Wuhan University, Wuhan, 430071 Hubei, People's Republic of China

5 Department of Physiology and Pharmacology, The University of Georgia, Athens, GA 30602, USA

Introduction

Myocardial ischemia or infarction is one of the main causes of heart failure. Myocardial infarction (MI) is usually initiated by myocardial ischemia resulting from the narrowing of coronary arteries due to atherosclerosis. Clinically, a number of cardiovascular intervention techniques such as thrombolytic therapy, percutaneous coronary intervention, and cardiac bypass surgery can restore myocardial perfusion. However, if the coronary flow is not restored within

1 ~ 2 h after the MI, reperfusion itself may cause harmful effects in the ischemic heart, a phenomenon known as reperfusion injury (I/R) [1, 2]. One of the factors causing damage is the over-production of reactive oxygen species (ROS). The ROS release subsequently causes extensive cardiomyocyte death and acute heart dysfunction [3]. ROS-caused apoptotic damages include membrane lipid peroxidation, protein cross-linking and degradation, DNA nicking, and mitochondria damage [4]. Blockade of oxidative stress-induced injury is therefore beneficial for the protection of cardiomyocytes.

Vascular endothelial growth factor (VEGF) family comprises five isoforms A, B, C, D, and E, and is known to promote vasculogenesis and angiogenesis [5]. In addition to angiogenesis, VEGF-A and its receptor play important roles in repairing ischemic or infracted heart through inducing cardiac stem cell differentiation and migration [6]. VEGF-C,an important member of VEGF family [7], has been characterized as a lymphangiogenic and angiogenic growth factors. VEGF-C functions through three VEGF-C receptor subtypes, VEGFR-2 (KDR/Flk-1), VEGFR-3 (Flt-4), and NRP-2 [8–10]. VEGF-C is significantly up-regulated in both early and late stages of MI [11]. However, it is unknown if VEGF-C plays a role in ROS-induced cardiomyocyte injury.

Two distinct apoptotic pathways are reported to direct cell apoptosis: a death receptor-mediated pathway and an intrinsic pathway in which mitochondria play a central role in assimilating and affecting various apoptotic signals [8]. H_2O_2 is reported to induce cardiomyocyte apoptosis through mitochondria-dependent pathway [4]. In the present study, we found that VEGF-C promoted rat cardiomyocyte survival through VEGFR-2 under oxidative stress conditions. The underlying molecular mechanism of VEGF-C involves the activation of PI3k/Akt signaling and blockade of mitochondria apoptotic pathway.

Materials and methods

All animal experiments were performed according to the *Guide for the Care and Use of Laboratory Animals* recommended by the National Institutes of Health of USA. All protocols of animal studies were approved by the Institutional Animal Care and Use Committee of Hubei University of Medicine.

Heart ischemia–reperfusion injury model

Myocardial ischemia–reperfusion injury (I/R) in rats was performed as previously described [12]. Briefly, Sprague–Dawley rats (240 ± 35 g, male) were randomly divided into four groups as follows: sham group, I/R group, VEGF-C (0.1 μg/kg b.w.) group, and VEGF-C (1.0 μg/kg b.w.) group. These rats were anesthetized with ketamine (50 mg/kg, b.w., ip) and xylazine (10 mg/kg b.w., ip) and ventilated during surgery using a Columbus ventilator (HX-300, Taimeng Instruments, China). 1 h after pre-treatment with VEGF-C (local injection of myocardium), the hearts were ligated on the left anterior descending coronary artery (LAD) for 1 h before reperfusion for 24 h. Buprenorphine hydrochloride (0.05 mg/kg, sc) was administered one time after the procedure.

Measurement of hemodynamics

Hemodynamic measurement was carried out using protocol published in our previous study [12]. Briefly, 24 h after reperfusion, left carotid artery was exposed. The heparinized (10 U/ml) catheter was inserted into the left ventricle to monitor hemodynamic parameters including left ventricle systolic pressure (LVSP), left ventricle end-diastolic pressure (LVEDP), and rates of the rise or fall of left ventricular pressure ($\pm dp/dt_{max}$) through signal conversion of pressure transducer (Chengdu taimeng Technology Co., Ltd, China) linked into BL-420S (Chengdu taimeng Technology Co., Ltd, China) for 15 min.

Measurement of the infarcted sizes

The infarcted sizes were analyzed as previously described [6]. Briefly, each heart was cut into 5 sections with a thickness of 2–5 mm each section. 1 % 2, 3, 5-triphenyltetrazolium chloride (TTC, Sigma, USA) was used to stain the heart sections at 37 °C for 15 min. The infracted size was calculated and expressed as a percentage of the area of infarcted LV myocardium unstained by TTC in the total area of LV myocardium stained and unstained by TTC.

Biochemical detection

Measurement of creatine kinase (CK), CK-MB activity, cardiac troponin T (cTnT), malondialdehyde (MDA), and lactate dehydrogenase (LDH) levels were performed as described in detail previously [12, 13]. Briefly, 24 h after treatment, blood samples were centrifuged at 3500 rpm for 15 min at 4 °C, then serum was collected. CK activities (JianCheng Bioengineering Institute, China), CK-MB activity (Rapidbio, USA), and cTnT (Rapidbio, USA) levels were analyzed using corresponding commercial kits by following the manufacture's instruction. MDA (an oxidative damage marker of myocardium) and LDH (an indicator of cellular injury) were detected by using commercial kits (JianCheng Bioengineering Institute, China).

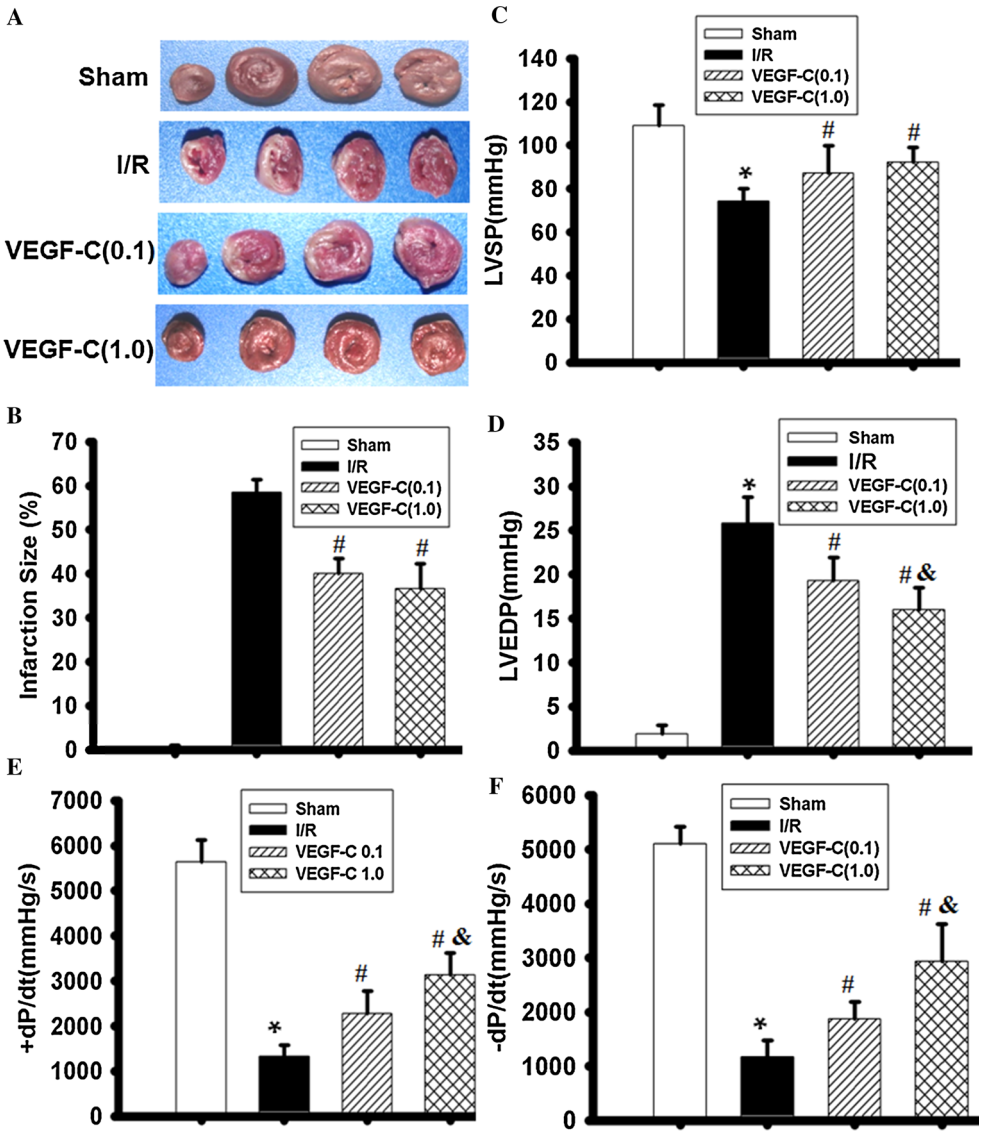

Fig. 1 VEGF-C improved heart function impaired due to I/R injury. **a** The TTC staining showing the infarcted myocardium 24 h after reperfusion. **b** Quantitative analysis of infarction size. $^{*}P < 0.01$ versus sham group; $^{\#}P < 0.01$ versus I/R group, $n = 6$. (**c**–**f**) Quantitative analysis of heart function including LVSP (**c**), LVEDP (**d**), $\pm dp/dt_{max}$ (**e**, **f**). $^{*}P < 0.01$ versus sham group; $^{\#}P < 0.05$ versus I/R; $^{\&}P < 0.05$ versus hearts with the injection of 0.1 μ kg b.w. of VEGF-C, $n = 6$

ROS detection

The levels of O_2^- in cells were detected with oxidation-sensitive fluorescent probe dihydroethidium (DHE) (Invitrogen, USA) and measured with fluorescent microscopy as described previously [13].

Culture of H9c2 rat cardiomyocytes

The rat embryonic ventricular myocardial cell line H9c2 was purchased from the Cell Bank of the Chinese Academy of Sciences (Shanghai, China). H9c2 cells were cultured in DMEM (Invitrogen, USA) with 5 g/l glucose supplemented with 15 % fetal bovine serum (FBS, Hangzhou Sijiqing Biological Engineering Materials Co., Ltd., China) in 10 cm cell culture dish at 37 °C with an atmosphere of 5 % CO_2. When the 70–80 % confluence of cells was reached, the cells were passaged or used for experiments. For inducing apoptosis, the cells were exposed to H_2O_2 (400 μM, Sigma-Aldrich, St Louis, MO, USA) for different times following VEGF-C treatment (20 ng/ml, Peprotech, USA).

Quantitative reverse transcription polymerase chain reaction (qRT-PCR)

Total RNA of rat H9c2 cells was extracted by using Trizol Reagent (Invitrogen). RNA concentration was measured by UV spectrophotometry. qRT-PCR was performed using THUNDERBIRD SYBR qPCR Mix (TOYOBO, Japan) on a real-time PCR detection system (Slan, Hongshi) with the following cycles: 95 °C for 1 min, followed by 95 °C for 15 s, 58 °C for 20 s, and 72 °C for 20 s for 40 cycles. β-actin was used as an internal control. Primer sequences

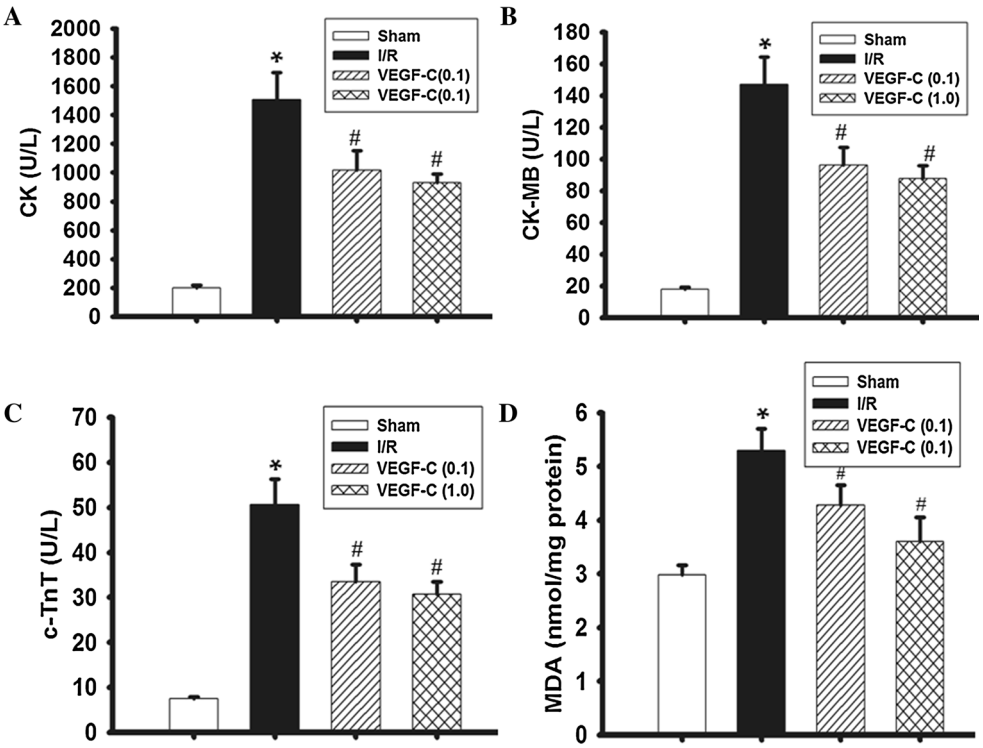

Fig. 2 VEGF-C suppressed CK, CK-MB, cTnT, and MDA levels in vivo. CK activity (**a**), CK-MB activity (**b**), cTnT level (**c**), and MDA levels (**d**) were analyzed as described in Materials and Methods. $^{*}P < 0.01$ versus sham group; $^{\#}P < 0.05$ versus I/R group, $n = 6$

were as follows: flk-1: 5′-ACC TAT CAA CTT ACT TAC GGG GC-3′ (forward), 5′-TCT GAC TGC TGG TGA TGC TGT-3′ (reverse); flt-4: 5′-TGA AAG ACG GCA CAC GAA TG-3′ (forward), 5′-CCT CGC TTT AGG GTC TCC AG-3′(reverse); nrp-2: 5′-GGC AGG TTT CTC CCT ACG CT-3′ (forward), 5′-TTT ACA GTC TCC TTC CCC CAC-3′ (reverse); and β-actin: 5′-CGT TGA CAT CCG TAA AGA CCT C-3′ (forward), 5′-TAG GAG CCA GGG CAG TAA TCT-3′ (reverse).

Immunofluorescent staining of VEGF-C receptors

To detect VEGF-C receptors in H9c2 cells, cells were cultured to 50–60 % confluence in the 8-well chamber slide (Lab-Tek® Chamber Slide™ System, NUNC, USA). Cells were fixed with 4 % paraformaldehyde for 1 min, washed three times with PBS followed by permeabilization with 0.2 % Triton X-100 for 5 min, and blocked using 10 % goat serum dissolved in PBS for 30 min at room temperature. Cells were then incubated with polyclonal anti-Flk-1, anti-Flt-4, and anti-neuropilin-2 IgG (diluted 1:50 in blocking buffer, Santa Cruz, USA) at 4 °C overnight followed by incubation with FITC-conjugated secondary antibodies (1:100, Santa Cruz) at room temperature for 1 h. After washing twice, cells were stained with Hoechst 33258 (2.5 μg/ml, sigma) in a dark chamber at room temperature for 20 min. The immunostaining of VEGF receptors was observed using a fluorescence microscope.

Cell viability and apoptosis assay

Cell viability was determined using Cell Counting Kit-8 as described previously [14]. H9c2 cell apoptosis was detected using Annexin V and Propidium Iodide (PI) binding Assay (Bender MedSystems, Austria) as described previously [12]. The apoptotic H9c2 cells were observed using a fluorescence microscope. In vivo cardiomyocyte apoptosis was detected using an In Situ Apoptosis Detection Kit (MM_NF-S7165#, Millipore, UEA) as described previously [4].

Measurement of mitochondrial membrane potential

Mitochondrial transmembrane potential was analyzed using a sensitive fluorescent probe, JC-1 (Invitrogen, USA) as described previously [15]. In brief, H9c2 cells were cultured in the 8-well chamber slide (Lab-Tek® Chamber Slide™ System, NUNC, USA) followed by appropriate treatments. The cells were then incubated with 5 μm of JC-1 in fresh culture medium at 37 °C for 15 min. JC-1 fluorescence was immediately detected and imaged under a fluorescent microscope.

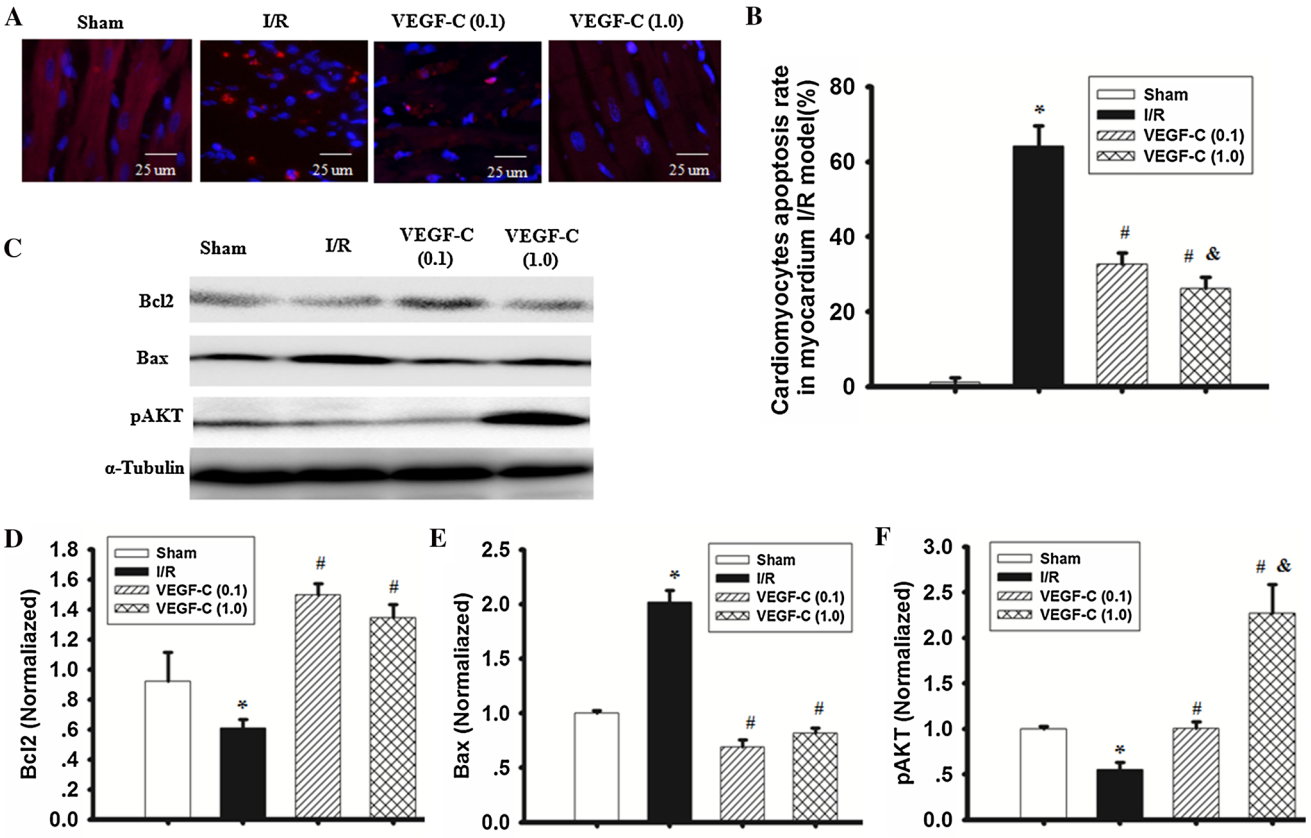

Fig. 3 VEGF-C inhibited I/R-mediated cardiomyocyte apoptosis through PI3K/Akt signaling. **a** Cardiomyocyte apoptosis in heart I/R model was detected by TUNNEL staining. *Red fluorescence* apoptotic cells; *Blue fluorescence* nuclei. **b** Quantitative analysis of cell apoptosis rate in (**a**). $^{*}P < 0.01$ versus sham group; $^{\#}P < 0.05$ versus I/R group; $^{\&}P < 0.05$ versus hearts with the injection of 0.1 μ kg b.w. of VEGF-C, $n = 6$. **c** Bcl-2, Bax and pAkt levels were detected by Western blot. **d**–**f** Quantification of Bcl-2, Bax, and pAkt expression by normalizing to α-Tubulin. $^{*}P < 0.01$ versus sham group; $^{\#}P < 0.05$ versus I/R group; $^{\&}P < 0.05$ versus hearts with the injection of 0.1 μ kg b.w. of VEGF-C, $n = 6$

Detection of intracellular cytochrome C localization

Cytochrome C release from the mitochondria was analyzed using MitoTracker Red CMXRos dye (Molecular Probes, USA) as described previously [16]. In brief, H9c2 cells were cultured in the 8-well chamber slide (Lab-Tek® Chamber Slide™ System, NUNC, USA) followed by appropriate treatments. The cells were incubated with 20 nM MitoTracker Red CMXRos dye at 37 °C for 15 min, fixed with 4 % paraformaldehyde for 15 min, washed three times with PBS followed by permeabilizing with 0.2 % Triton X-100 for 5 min, and blocked using 10 % goat serum dissolved in PBS at room temperature for 30 min. Cells were then incubated with monoclonal anti-cytochrome C IgG (diluted 1:50 in blocking buffer, Santa Cruz) at 4 °C overnight followed by incubation with FITC-conjugated goat anti-mouse IgG (1:100, Santa Cruz) at room temperature for 1 h. After washing twice, cells were observed under a fluorescence microscope.

Detection of Bax N-terminal exposure

Bax N-terminal epitope in mitochondrial membrane was analyzed using anti-Bax N-terminal (N20) IgG as described previously [16]. The cells were cultured in the 8-well chamber slide (Lab-Tek® Chamber Slide™ System, NUNC, USA) similarly as described in the detection of cytochrome C release. Cells were then incubated with anti-Bax N-terminal antibody (1:50, Santa Cruz) at 4 °C overnight followed by incubation with FITC-conjugated anti-rabbit IgG (1:50, Santa Cruz) at room temperature for 1 h. Bax conformational changes were observed under a fluorescence microscope.

Western blot

Western blot analysis was carried out as described previously [6]. The following primary antibodies were used: rabbit anti-Akt (#9272s, Cell Signaling Technology, 1:1000), rabbit anti-phospho-Akt (#9271s, Cell Signaling

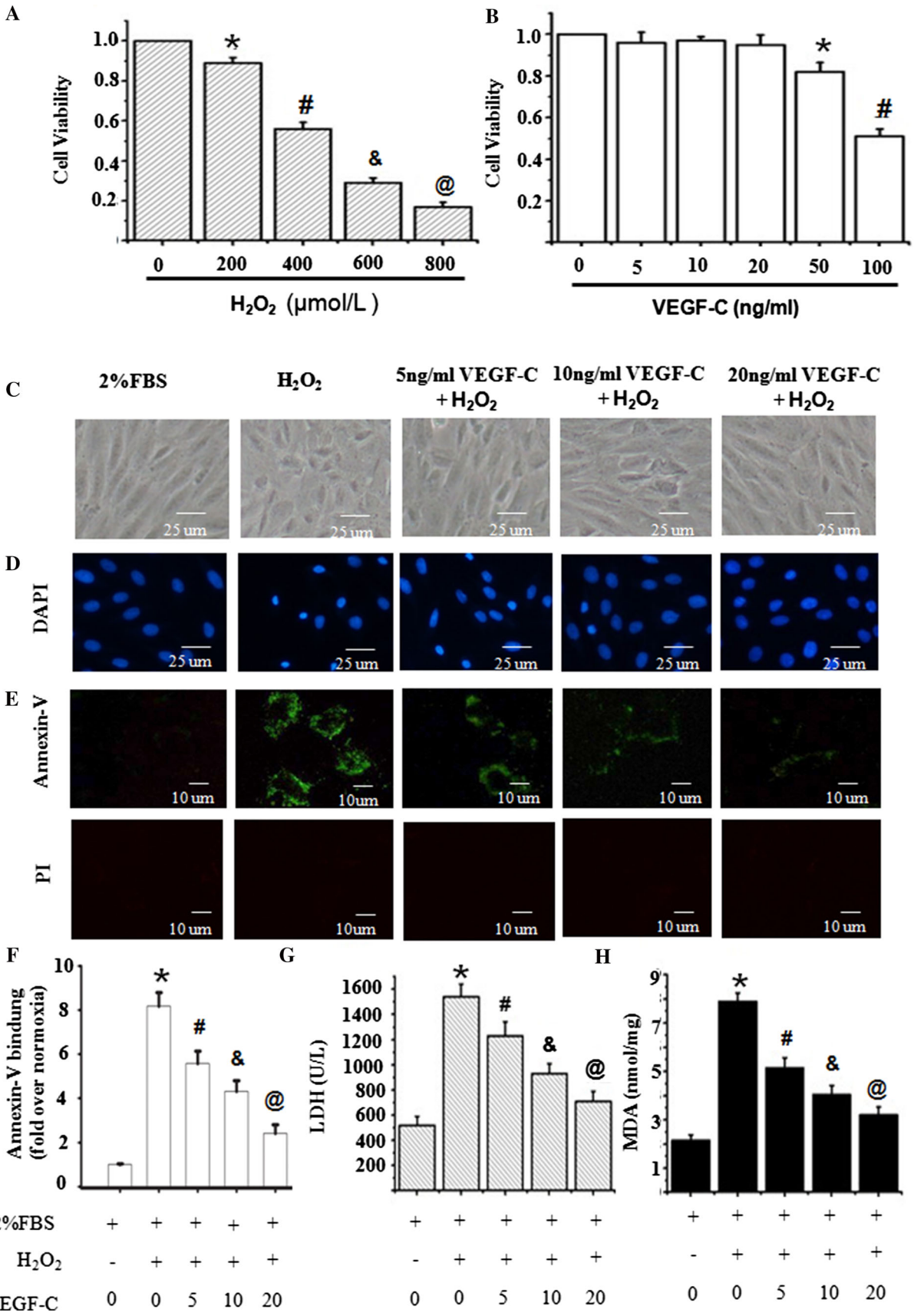
A
Cell Viability
1.0
0.8
0.6
0.4
0.2
*
#
&
@
0
200
400
600
800
H2O2 (μmol/L)
B
Cell Viability
1.0
0.8
0.6
0.4
0.2
*
#
0
5
10
20
50
100
VEGF-C (ng/ml)
C
2%FBS
H2O2
5ng/ml VEGF-C + H2O2
10ng/ml VEGF-C + H2O2
20ng/ml VEGF-C + H2O2
25 um
D
DAPI
25 um
E
Annexin-V
PI
10 um
F
Annexin-V bindung (fold over normoxia)
10
8
6
4
2
0
*
#
&
@
G
LDH (U/L)
1600
1400
1200
1000
800
600
400
200
*
#
&
@
H
MDA (nmol/mg)
9
7
5
3
1
*
#
&
@
2%FBS + + + + +
H2O2 - + + + +
VEGF-C 0 0 5 10 20

◀**Fig. 4** VEGF-C restored H_2O_2-induced alteration of H9C2 cell morphology while inhibiting H_2O_2-induced LDH release and MDA production. **a** Cell viability with H_2O_2 treatments was measured by CCK-8 assay. $^{*}P < 0.01$ versus 0 μM; $^{\#}P < 0.01$ versus 200 μM; $^{\&}P < 0.01$ versus 400 μM; $^{@}P < 0.01$ versus 800 μM H_2O_2-treated groups, $n = 3$. **b** Cell viability with VEGF-C treatment was measured by CCK-8 assay. $^{*}P < 0.01$ versus 0–20 ng/ml; $^{\#}P < 0.05$ versus 50 ng/ml VEGF-C-treated group. **c** Alterations of cell morphology were observed under light microscope 24 h after VEGF-C treatment (5–20 ng/ml) prior to treatment with 400 μM H_2O_2. **d** The condensed nuclei in apoptotic cells were stained with Hoechst 33258 and visualized under a fluorescence microscopy. **e** Cell apoptosis was detected by Annexin V/PI staining. **f** Quantitative analysis of cell apoptosis in (**e**). **g** VEGF-C reduced LDH levels. **h** VEGF-C decreased MDA levels. For **f–g**: $^{*}P < 0.01$ versus control (CTRL) for 2 % FBS-treated group; $^{\#}P < 0.05$ versus H_2O_2 group; $^{\&}P < 0.05$ versus 5 ng/ml of VEGF-C treatment group; $^{@}P < 0.05$ versus 10 ng/ml VEGF-C treatment group. $n = 6$

Technology, 1:1000), rabbit anti-Bax (#2772s, Cell Signaling Technology, 1:1000), rabbit anti-Bcl2 (#2876s, Cell Signaling Technology, 1:1000), or mouse anti-α-Tubulin antibody (Sigma, 1:5000). The corresponding horseradish peroxidase-conjugated anti-mouse and anti-rabbit secondary antibodies (1:10,000 dilution; Santa Cruz) were used. The immunoblots were detected by enhanced chemiluminescence reaction (Sigma).

Statistical analysis

All results are expressed as mean ± SD. Differences of parameters between two groups were evaluated by unpaired *t* test. Differences of parameters among more than two experimental groups were evaluated by one-way analysis of variance. *P* values <0.05 were considered statistically significant.

Results

VEGF-C reduced infarct size and improved heart function

To observe the effect of VEGF-C on myocardial infarct size in I/R model in vivo. 1 % TTC staining was used to evaluate infarct size of rat hearts undergoing I/R injury with or without VEGF-C treatment. We found that 0.1 and 1.0 μg/kg b.w. of VEGF-C treatment obviously decreased infarct size compared to the I/R-injured heart with vehicle treatment. 1.0 μg/kg b.w. of VEGF-C achieved a greater decrease of infarct size than 0.1 μg/kg b.w. of VEGF-C (Fig. 1a, b). Consistent with the reduction of the infarct size, left ventricle function in VEGF-C-treated animals was significantly improved. It was apparent that the higher dose of VEGF-C produced a much greater effect on the increase of LVSP and $\pm dp/dt_{max}$ along with the decrease of LVEDP than the lower dose of VEGF-C (Fig. 1c–f).

VEGF-C suppressed the activities of CK and CK-MB, reduced the levels of cTnT and MDA, and inhibited I/R-mediated cardiocytes apoptosis through PI3K/Akt signaling

To explore the role of VEGF-C in myocardium ischemia reperfusion (I/R) injury, CK and CK-MB activities as well as cTnT and MDA levels were detected to evaluate the myocardial injury. As shown in Fig. 2a–d, although I/R injury increased the CK and CK-MB activities and the cTnT and MDA levels, VEGF-C treatment significantly reversed the effect of I/R injury.

To determine how VEGF-C protects heart from I/R injury, cells apoptosis was first detected 24 h after VEGF-C treatment. As shown in Fig. 3a, b, VEGF-C significantly decreased the apoptosis rate of cardiomyocytes in I/R-injured hearts. Bcl-2, a marker for the survival of cardiocytes, and Bax, a marker of cardiocytes apoptosis [17, 18], were then used to evaluate the effect of VEGF-C on myocardium protection. Bcl-2 was markedly induced, and Bax was significantly inhibited in VEGF-C-treated hearts compared to the I/R-injured hearts with saline injection ($P < 0.05$). Importantly, Akt signaling as shown by Akt phosphorylation was obviously increased in VEGF-C-treated hearts (Fig. 3c–e). The higher dose of VEGF-C appeared to induce a much greater activation of the Akt signaling. These data suggest that VEGF-C may inhibit I/R-caused cardiomyocyte apoptosis through PI3K/Akt signaling.

VEGF-C protected H9c2 cells from H_2O_2 damage

Since ROS production is a major factor in I/R-induced myocardial infarction, we evaluated the protective effect of VEGF-C on H_2O_2-treated H9c2 cells. The H9c2 cell viability was gradually decreased when H_2O_2 concentration was increased (Fig. 4a). 50 or 100 ng/ml of VEGF-C significantly decreased the cell viability as shown by the CCK-8 assay (Fig. 4b). H_2O_2 has been shown to alter H9c2 cell morphology from the well organized and rod-like cell morphology to irregular morphology [19]. However, VEGF-C treatment restored the morphology of H9c2 cells (Fig. 4c). In addition, VEGF-C prevented H9c2 cells from producing the condensed nuclei induced by H_2O_2 (Fig. 4d). Meanwhile, VEGF-C attenuated the H_2O_2-induced phosphatidylserine (PS) production as shown by the Annexin V staining (Fig. 4e, f). The appearance of PS in the outer leaflet of the phospholipid bilayer without disrupted integrity of the membrane is one of the earliest characteristics of apoptotic process [15]. These data suggest that VEGF-C inhibited H_2O_2-induced apoptosis.

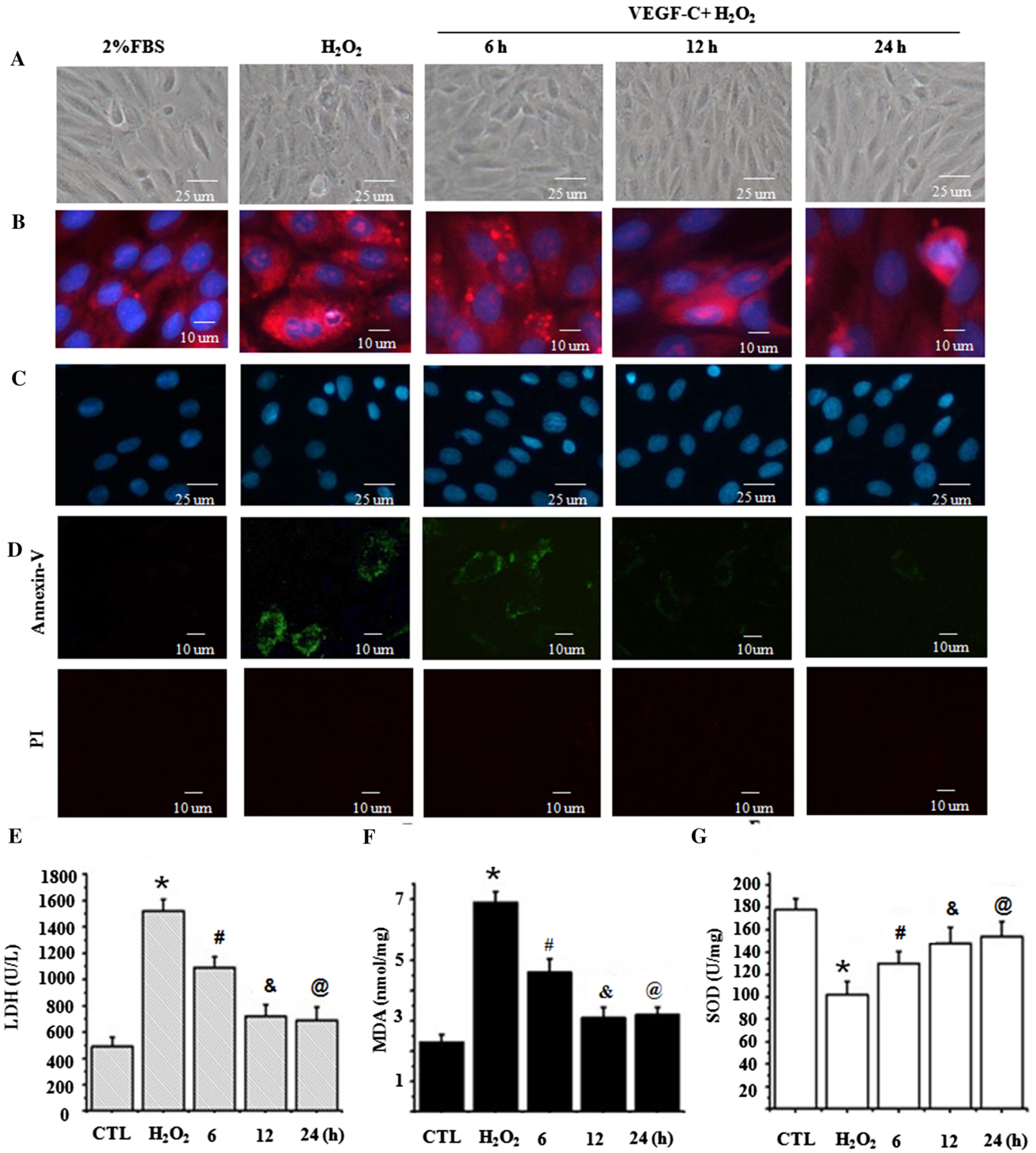

Fig. 5 Time-course protective effect of VEGF-C on H_2O_2-induced H9c2 cell apoptosis. **a** Effect of VEGF-C on H9c2 cell morphology. **b** O_2^- levels were detected by fluorescent microscopy. *Red color* was indicated as the changes of O_2^- levels in cells detected with oxidation-sensitive fluorescent probe dihydroethidium (DHE), *Blue color* was indicated as cell nucleus by DAPI staining. **c** The condensed nuclei in apoptotic cells were visualized by Hoechst 33258. **d** Cell apoptosis was detected by Annexin V/PI staining. **e** VEGF-C reduced LDH levels. **f** VEGF-C reduced MDA levels. **g** VEGF-C restored SOD levels. $^*P < 0.01$ versus 2 % FBS (CTRL) group; $^{\#}P < 0.05$ versus H_2O_2 treatment group; $^{\&}P < 0.05$ versus pre-treatment with VEGF-C for 6 h; $^{@}P > 0.05$ versus pre-treatment with VEGF-C for 12 h; $n = 6$ for each assay

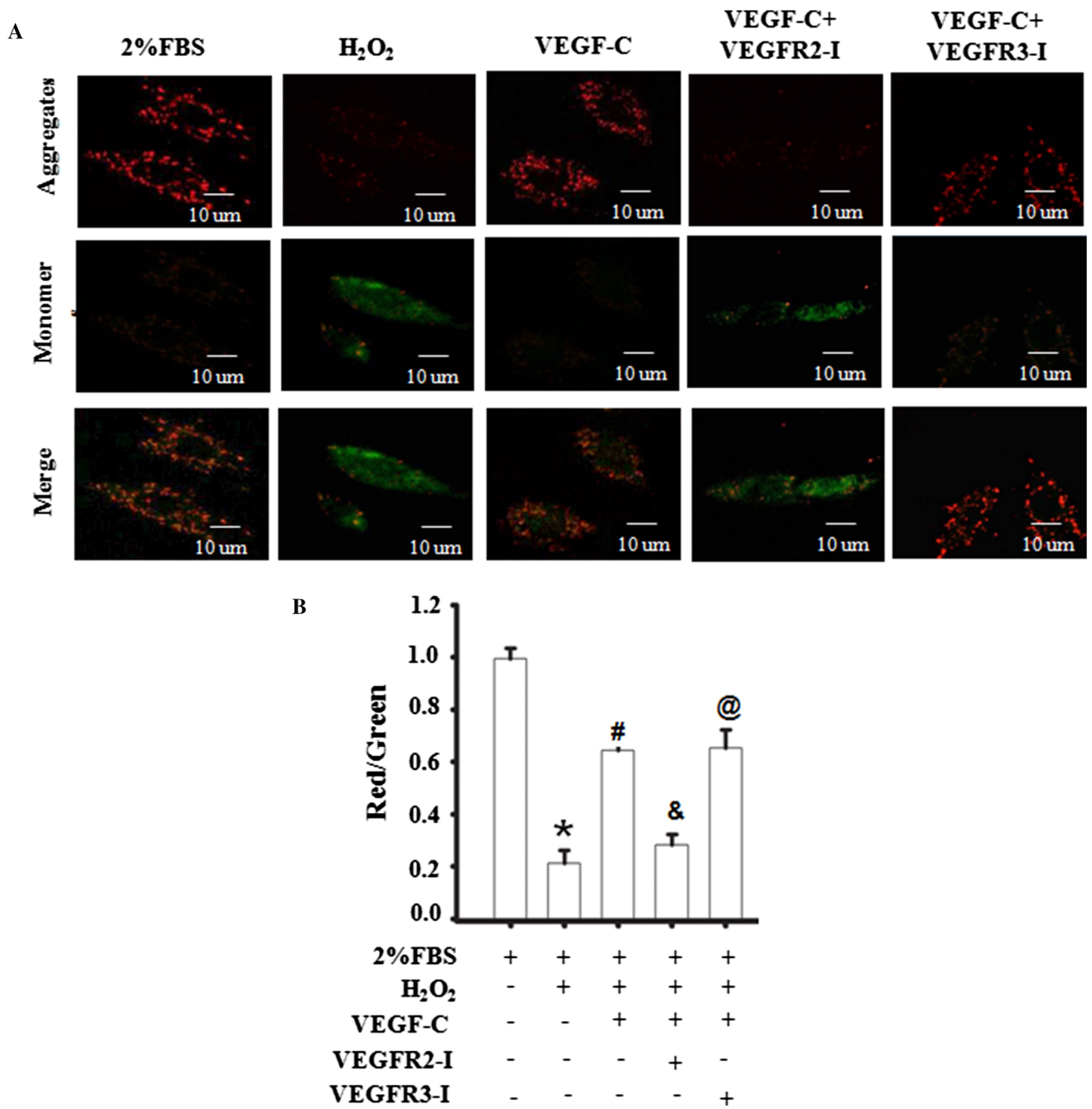

Fig. 6 VEGF-C restored H_2O_2-induced reduction of mitochondrial membrane potential via VEGFR2. **a** The lipophilic cationic probe JC-1 was used to analyze the alterations of mitochondrial transmembrane potential (MTP). JC-1 aggregates in mitochondria show *red color*, JC-1 monomers display *green* signal, indicator of the loss of MTP. **b** Quantitative analysis of MTP in (**a**). $^{*}P < 0.01$ versus 2 % FBS (CTRL) group; $^{\#}P < 0.05$ versus H_2O_2 treatment group; $^{\&,\ \$}P < 0.05$ versus VEGF-C pre-treatment group; $^{@}P > 0.05$ versus VEGF-C pre-treatment group; $n = 6$. VEGFR2-I: VEGFR2 inhibitor; VEGFR3-I: VEGFR3 inhibitor

LDH level is considered as a typical marker for cellular damage, and MDA is an indicator of cell oxidative injury. Compared to normal cells, LDH releases and MDA contents were obviously increased by oxidative injury (Fig. 4g, h). VEGF-C treatment, however, dose dependently decreased H_2O_2-induced LDH release and MDA contents (Fig. 4g, h).

To further test the role of VEGF-C in protecting H_2O_2-caused damage to cardiomyocytes, we treated H9c2 cells with VEGF-C for 6, 12, and 24 h and found that VEGF-C

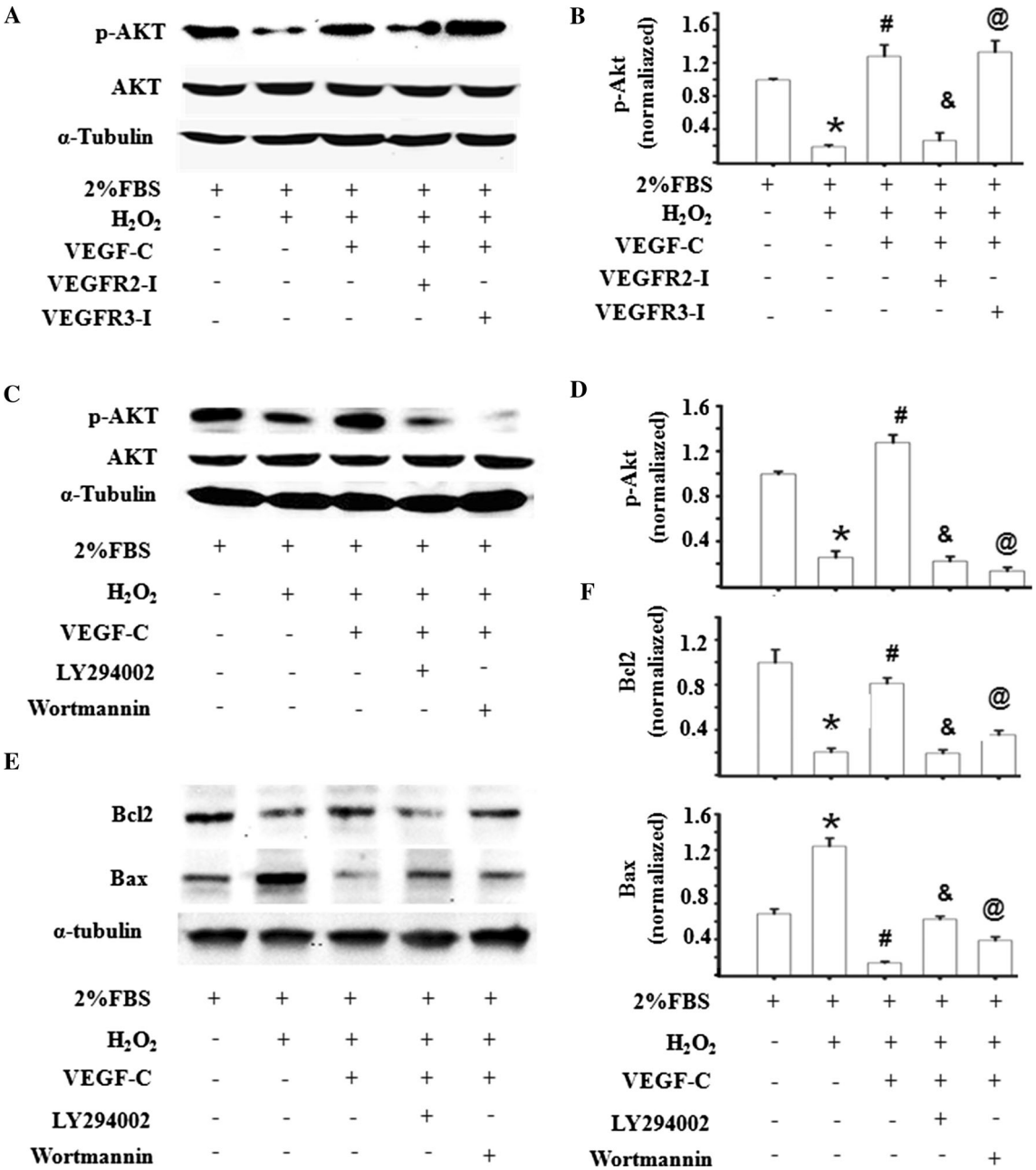

Fig. 7 VEGF-C regulated Bcl2/Bax expression via PI3/Akt signaling. **a** VEGF-C restored H_2O_2-blocked Akt phosphorylation via PI3K signaling. Akt phosphorylation and expression were analyzed by Western blot. α-tubulin served as an internal control. **b** Quantitative analysis of Akt phosphorylation by normalized to the total Akt level. **c** Bcl2 and Bax protein expression was detected by Western blot. **d** Quantification of Bcl2 and Bax expression by normalized to α-Tubulin. $^{*}P < 0.01$ versus 2 % FBS (CTRL) group; $^{\#}P < 0.05$ versus H_2O_2 treatment group; $^{\&,\ @}P < 0.05$ versus VEGF-C pre-treatment group; $n = 6$

restored H9c2 cell morphology (Fig. 5a), decreased ROS production (Fig. 5b), repaired the condensed nuclei (Fig. 5c), reduced the PS production (Fig. 5d), decreased the LDH release and MDA contents (Fig. 5e, f), and increased SOD expression (Fig. 5g) that was altered by H_2O_2 in time-dependent manners. These data further demonstrated that VEGF-C is able to protect cardiomyocytes from ROS-induced injury.

VEGF-C restored H_2O_2-blocked mitochondrial membrane potential

The mitochondrial membrane potential plays a crucial role in sustaining the entirety of mitochondria and subsequent regulation of apoptosis in response to injury stimuli. Loss of mitochondrial membrane potential activates the cytochrome c-initiated pathway to induce cell apoptosis [16].

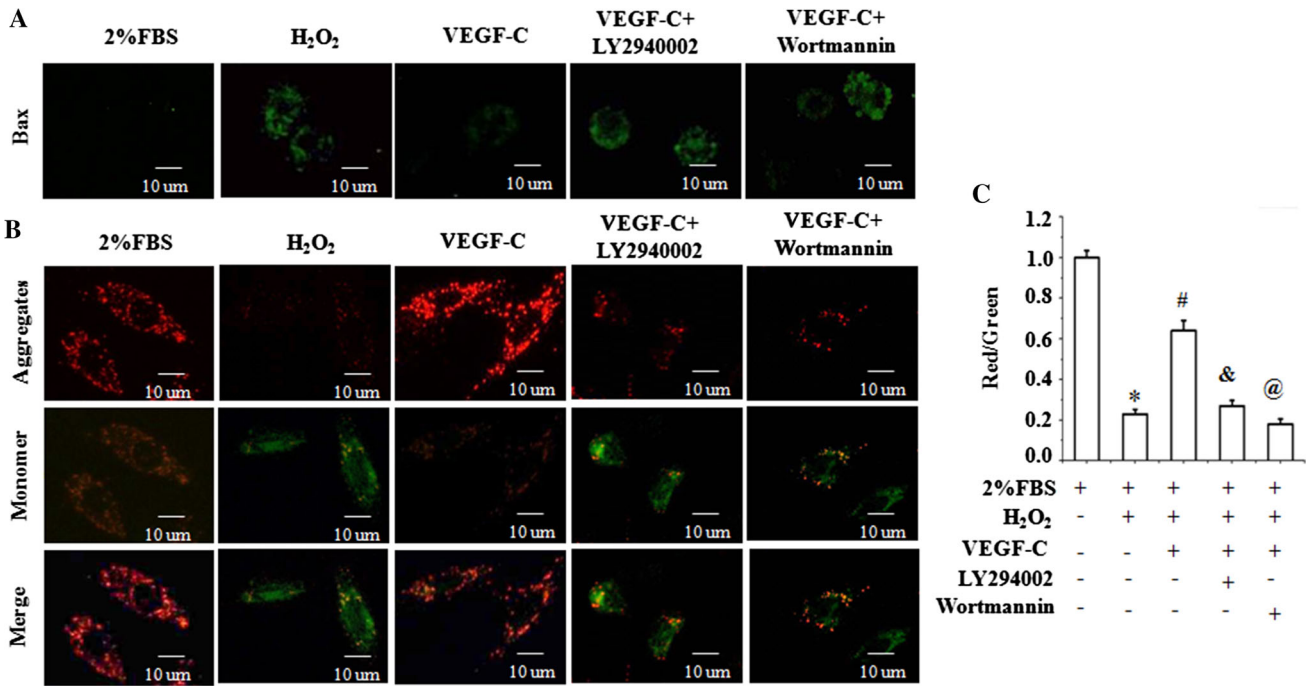

Fig. 8 VEGF-C inhibited H_2O_2-induced reduction of MTP through Bax translocation. **a** VEGF-C alleviated Bax translocation from cytoplasm to mitochondrial membrane induced by H_2O_2. **b** MTP was assessed by JC-1 aggregates. **c** Quantitative analysis of membrane potential in (**b**). $^{*}P < 0.01$ versus control (CTRL) group; $^{\#}P < 0.05$ versus H_2O_2 treatment group; $^{\&}P < 0.05$ versus VEGF-C pre-treatment group; $^{@}P < 0.05$ versus VEGF-C pre-treatment group; $n = 6$

JC-1, a specific indicator for mitochondrial membrane potential, can be used to assess mitochondria function by its different aggregations due to the switch between red and green color. Normal growing H9c2 cells exhibited a bright red fluorescence with the JC-1 incubation (Fig. 6a). H_2O_2 treatment reduced the red aggregates and generated significantly more JC-1 monomers as shown by the green fluorescence, indicating dissipation of the mitochondrial membrane potential. VEGF-C treatment, however, attenuated the H_2O_2-induced effects (Fig. 6a), suggesting that VEGF-C inhibits H_2O_2-induced apoptosis by restoring mitochondrial membrane potential.

VEGFR-2 mediated VEGF-C-induced mitochondria-protective effects

VEGF-C functions by activating its cognate tyrosine kinase receptors VEGFR2 (Flk-1), VEGFR3 (Flt-4), and/or the nontyrosine kinase receptor neuropilin-2 (NRP-2). We found that H9c2 cells mainly express Flk-1 with a low level expression of Flt-4 (Supplemental Figure S1). To determine whether Flk-1 or Flt4 is important for VEGF-C function, we blocked these two receptors in VEGF-C- and H_2O_2-treated H9c2 cells. As shown in Fig. 6a, b. Flk1 inhibitor, but not Flt4 inhibitor, blocked VEGF-C function and thus retained H_2O_2-induced reduction of red/green JC-1 aggregate ratio. These data indicated that VEGF-C functions through VEGFR-2 to exert the mitochondria-protective effects.

VEGF-C regulated Bcl2/Bax expression via PI3/Akt signaling

Apoptosis is mediated by numerous signaling pathways such as PI3K/Akt and p38 MAPK [20, 21]. To determine if VEGF-C affects PI3K/Akt signaling, we examined the activation of PI3K/Akt signaling. VEGF-C increased Akt phosphorylation that was reduced by H_2O_2 but did not affect its expression, which was blocked by Flk1 inhibitor, but not Flt4 inhibitor, suggesting that VEGF-C induced the increase of pAkt levels through VEGFR2 (Fig. 7a, b). Subsequently, PI3K-specific inhibitor wortmannin or LY294002 was used to analyze VEGF-C-mediated activation of PI3K/Akt signaling, we found that both wortmannin and LY294002 could abolish the specific effects of VEGF-C on Akt phosphorylation (Fig. 7c, d). Since cell survival regulators Bcl2 and Bax are regulated by PI3K/Akt signaling, we tested if VEGF-C regulates Bcl2 and Bax expression. As shown in Fig. 7e, f, VEGF-C reversed the effect of H_2O_2 and thus markedly increased Bcl-2, while decreased Bax expression suggesting that VEGF-C protected H9c2 cells from H_2O_2-induced apoptosis via augmenting Bcl-2 while suppressing Bax expression. Wortmannin or LY294002 blocked VEGF-C-mediated

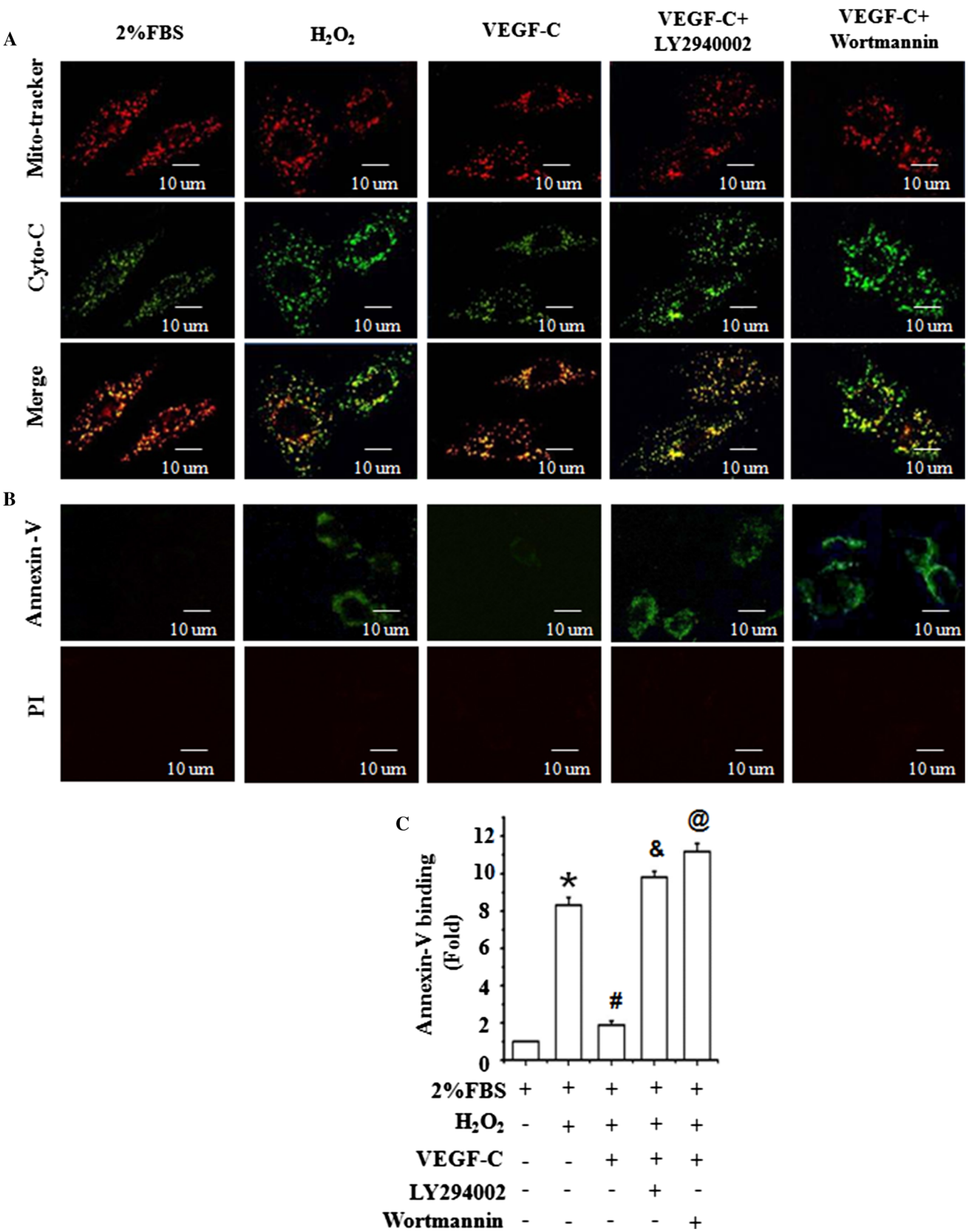
A
2%FBS
H2O2
VEGF-C
VEGF-C+ LY2940002
VEGF-C+ Wortmannin
Mito-tracker
Cyto-C
Merge
10 um
B
Annexin-V
PI
C
Annexin-V binding (Fold)
12
10
8
6
4
2
0
*
#
&
@
2%FBS + + + + +
H2O2 - + + + +
VEGF-C - - + + +
LY294002 - - - + -
Wortmannin - - - - +

◀**Fig. 9** VEGF-C restored H_2O_2-induced cytochrome c release via PI3k signaling. **a** VEGF-C reduced cytochrome c release from mitochondria in response to H_2O_2. *Red* signal indicates mitochondria by mitotracker staining, green signal shows cytochrome c staining, and *yellow* in merged images indicates localization of cytochrome c in mitochondria. **b** Cell apoptosis was measured by Annexin V/PI staining. **c** Quantitative analysis of apoptosis cell in **b**. $^{*}P < 0.01$ versus control (CTRL) group; $^{\#}P < 0.05$ versus H_2O_2 treatment group; $^{\&}P < 0.05$ versus VEGF-C pre-treatment group; $^{@}P < 0.05$ versus VEGF-C pre-treatment group; $n = 6$

Bcl2 and Bax expression, suggesting that VEGF-C regulates Bcl2/Bax expression through PI3/Akt signaling pathway.

VEGF-C inhibited H_2O_2-induced reduction of mitochondrial membrane potential through Bax translocation

The pro-apoptotic protein Bax causes the loss of mitochondrial membrane potential and damages mitochondrial function by its translocation from cytoplasm to mitochondrial membrane [22]. To determine if VEGF-C protects H_2O_2-induced damage via Bax mitochondrial translocation, we observed the exposure of Bax N-terminal domain on mitochondrial membrane by immunostaining. In normal cells, no Bax N-terminal was present on mitochondria. H_2O_2 treatment induced a significant exposure of Bax N-terminal domain as shown by green fluorescent signal (Fig. 8a). However, this effect was clearly inhibited by VEGF-C treatment (Fig. 8a). Interestingly, the effect of VEGF-C on Bax translocation was blocked by PI3 kinase-specific inhibitor Wortmannin or LY294002, suggesting that VEGF-C recovered mitochondrial function through blocking Bax translocation, which was mediated by PI3K signaling.

To further explore the involvement of mitochondria in VEGF-C function, we also tested if the effect of VEGF-C on mitochondrial membrane potential involves PI3K signaling by immunostaining the JC-1. As shown in Fig. 8b, c, VEGF-C evidently increased the JC-1 aggregates shown in red and decreased JC-1 monomers in the cytoplasm, and these special effects were abolished by LY294002 or Wortmannin, suggesting that PI3K signaling plays a critical role in VEGF-C-mediated restoration of mitochondrial function such as mitochondrial membrane potential in H9c2 cells that were impaired by ROS.

Together, these data demonstrated that VEGF-C protects cardiomyocytes from ROS-induced injury through inhibiting cardiomyocyte apoptosis, which is achieved by blocking Bax mitochondrial translocation via PI3 kinase signaling pathway.

VEGF-C inhibited H_2O_2-induced cytochrome c release via PI3K/Akt Signaling

Cytochrome c Release from mitochondria is another indicator of intracellular apoptotic signaling activation and subsequent cell death in response to injury stimuli [23]. H_2O_2 treatment induced cytochrome c release from mitochondria, as shown by the loss of co-localization between cytochrome c and mitochondria (Fig. 9a). The effect of H_2O_2 was alleviated by pre-treatment with VEGF-C (Fig. 9a). However, when PI3 kinase signaling was blocked by LY294002 or Wortmannin, VEGF-C-inhibited apoptosis shown by Annexin V staining was diminished, confirming that VEGF-C inhibited H_2O_2-induced cytochrome c release through activating PI3k signaling (Fig. 9b, c).

Discussion

Myocardial I/R injury causes complications such as decreased cardiac contractile function and arrhythmias [24]. Oxidative stress is one of the major factors causing I/R injury, and many of the therapies targeting the reduction of this stress in vivo are proven to be of clinically benefit [25, 26]. VEGF-C is increased in the infarcted heart in both early and late stages of MI [11]. In the present study, we demonstrate for the first time that VEGF-C protects cardiomyocytes from oxidative stress-induced apoptosis in vitro and I/R-induced apoptosis in vivo, suggesting that the VEGF-C induced during the MI is for the protection of the infracted heart. VEGF-C appears to prevent the activation of mitochondria apoptotic pathway through activating PI3k/Akt signaling pathway.

VEGF regulates the function of cardiovascular system through binding in an overlapping pattern to three receptor tyrosine kinases (RTKs), known as VEGF receptor-1, -2, and -3 (VEGFR1-3), as well as co-receptors NRP2 [27, 28]. VEGF-C appears to exert its protective effect by binding to VEGFR2 because only VEGFR2 is expressed at a high level in H9c2 cell, while other receptors or NRP-2 is barely detectable. Moreover, blocking VEGFR2 by its inhibitor significantly inhibits VEGF-C protective effect, demonstrating that VEGFR2 mediates VEGF-C function in cardiomyocytes.

Previous studies have suggested that mitochondrion plays an important role in the determination of cells fates such as cells survival or apoptosis in response to stress [26]. Herein, VEGF-C maintains cardiomyocyte survival by reversing ROS-induced nuclear condensation, disruption of membrane integrity, loss of mitochondrial membrane potential, and release of cytochrome c. Mechanistically, VEGF-C prevents the activation of the intrinsic pathway of apoptosis by preventing H_2O_2-induced

mitochondria localization and activity of the pro-apoptotic Bax protein, leading to mitochondrial membrane potential restoration and inhibition of subsequent cytochrome c release. These results implied that VEGF-C blocks apoptosis in cardiomyocyte through inhibiting the mitochondria apoptotic pathway.

Previous studies have also shown that VEGF has a pro-survival function of cells [29]. Herein, VEGF-C increases Akt activation in cardiomyocytes both in vitro and in vivo, and these special effects are abolished by PI3K inhibitors, suggesting that the protective effect of VEGF-C on cardiomyocytes is dependent of PI3/Akt signaling. Interestingly, PI3K inhibitors wortmannin and LY294002 have been shown to cause endothelial cell apoptosis by significantly increasing caspase-3 activity in the presence of exogenous VEGF-A [28, 30]. Furthermore, a critical pathway of caspase activation is the cytochrome c-initiated pathway [31]. In this study, the effects of VEGF-C on Bcl2/Bax expression, mitochondria membrane potential, and cytochrome c release in cardiomyocytes are all abolished by wortmannin or LY294002, demonstrating that VEGF-C prevents the activation of the intrinsic apoptotic pathway through PI3K/Akt signaling pathway.

Importantly, consistent with the effect of VEGF-C in H_2O_2-induced apoptosis of cardiomyocytes in vitro, VEGF-C induces an increase in Bcl-2 level and a decrease in Bax level, suggesting that heart following I/R in vivo may be benefited more by VEGF-C treatment than the factors only affecting a single apoptosis-related protein.

Interestingly, 50 ng and 100 ng/ml of VEGF-C reduces H9c2 cells viability, suggesting that high dose of VEGF-C can cause damage to cardiomyocytes. Indeed, VEGF-C has been found to promote hypertrophy of cardiomyocyte [32], and hypertrophying cardiomyocytes exhibit lower cell viability [33]. Therefore, overdosing VEGF-C may decrease cell viability by inducing cells hypertrophy.

Although VEGF-C promotes cardiomyocyte hypertrophy and survival [32, 34], but the molecular mechanisms remain to be studied. Our studies show that VEGF-C markedly decreases myocardiocyte apoptosis and the infarction size in I/R hearts, significantly improved LVSP and $\pm dp/dt_{max}$, and reduced LVDEP. Collectively, our results demonstrate that VEGF-C exerts a protective effect against I/R-induced and ROS-mediated apoptosis of cardiomyocytes by preventing activation of the mitochondrial-dependent intrinsic apoptotic pathway, via the activation of PI3K signaling.

Acknowledgments This study was supported by grants from the National natural Science Foundation of China (81170095 to J.M.T, 81328002 to S.Y.C), Hubei Department Science (2014CFB644 to J.M.T), Hubei Education Department Science Foundation (T201112 to J.M.T), and the National Institutes of Health (HL123302, HL119053, and HL107526 to S.Y.C.).

References

1. Ibáñez B, Heusch G, Ovize M, Van de Werf F (2015) Evolving therapies for myocardial ischemia/reperfusion injury. J Am Coll Cardiol 65:1454–1471
2. Reiter R, Swingen C, Moore L, Henry TD, Traverse JH (2012) Circadian dependence of infarct size and left ventricular function after ST elevation myocardial infarction. Circ Res 110:105–110
3. Hausenloy DJ, Yellon DM (2013) Myocardial ischemia–reperfusion injury: a neglected therapeutic target. J Clin Investig 123:92–100
4. von Harsdorf R, Li PF, Dietz R (1999) Signaling pathways in reactive oxygen species-induced cardiomyocyte apoptosis. Circulation 99:2934–2941
5. Ferrara N, Gerber HP, LeCouter J (2003) The biology of VEGF and its receptors. Nat Med 9:669–676
6. Tang JM, Wang JN, Zhang L (2011) VEGF/SDF-1 promotes cardiac stem cell mobilization and myocardial repair in the infarcted heart. Cardiovasc Res 91:402–411
7. Kajdaniuk D, Marek B, Foltyn W (2011) Vascular endothelial growth factor (VEGF): part 1: in physiology and pathophysiology. Endokrynol Pol 62:444–455
8. Dias S, Choy M, Alitalo K (2002) Vascular endothelial growth factor (VEGF)-C signaling through FLT-4 (VEGFR-3) mediates leukemic cell proliferation, survival, and resistance to chemotherapy. Blood 99:2179–2184
9. Karpanen T, Heckman CA, Keskitalo S (2006) Functional interaction of VEGF-C and VEGF-D with neuropilin receptors. FASEB J 20:1462–1472
10. Muders MH, Zhang H, Wang E (2009) Vascular endothelial growth factor-C protects prostate cancer cells from oxidative stress by the activation of mammalian target of rapamycin complex-2 and AKT-1. Cancer Res 69:6042–6048
11. Zhao T, Zhao W, Chen Y (2013) Differential expression of vascular endothelial growth factor isoforms and receptor subtypes in the infarcted heart. Int J Cardiol 167:2638–2645
12. Huang GQ, Wang JN, Tang JM, Zhang L, Zheng F, Yang JY, Guo LY, Kong X, Huang YZ, Liu Y, Chen SY (2011) The combined transduction of copper, zinc-superoxide dismutase and catalase mediated by cell-penetrating peptide, PEP-1, to protect myocardium from ischemia–reperfusion injury. J Transl Med 9:73
13. Mishra V, Baines M, Wenstone R (2005) Markers of oxidative damage, antioxidant status and clinical outcome in critically ill patients. Ann Clin Biochem 42:269–276
14. Hou G, Xue L, Lu Z (2007) An activated mTOR/p70S6 K signaling pathway in esophageal squamous cell carcinoma cell lines and inhibition of the pathway by rapamycin and siRNA against mTOR. Cancer Lett 253:236–248
15. Shin EJ, Schram K, Zheng XL (2009) Leptin attenuates hypoxia/reoxygenation-induced activation of the intrinsic pathway of apoptosis in rat H9c2 cells. J Cell Physiol 221:490–497
16. Eguchi M, Liu Y, Shin EJ (2008) Leptin protects H9c2 rat cardiomyocytes from H_2O_2-induced apoptosis. FEBS J 275:3136–3144
17. Cook SA, Sugden PH, Clerk A (1999) Regulation of bcl-2 family proteins during development and in response to oxidative stress in cardiac myocytes: association with changes in mitochondrial membrane potential. Circ Res 85:940–949
18. Valks DM, Kemp TJ, Clerk A (2003) Regulation of Bcl-xL expression by H_2O_2 in cardiac myocytes. J Biol Chem 278:25542–25547
19. Lee YS, Kang YJ, Kim HJ (2006) Higenamine reduces apoptotic cell death by induction of hemeoxygenase-1 in rat myocardial ischemia–reperfusion injury. Apoptosis 11:1091–1100

20. Zhang L, Dong XW, Wang JN (2012) PEP-1-CAT-transduced mesenchymal stem cells acquire an enhanced viability and promote ischemia-induced angiogenesis. PLoS One 7:e52537
21. Desbiens KM, Deschesnes RG, Labrie MM, Desfossés Y, Lambert H, Landry J, Bellmann K (2003) c-Myc potentiates the mitochondrial pathway of apoptosis by acting upstream of apoptosis signal-regulating kinase 1 (Ask1) in the p38 signalling cascade. Biochem J 372:631–641
22. Hou Q, Hsu YT (2005) Bax translocates from cytosol to mitochondria in cardiac cells during apoptosis: development of a GFP-Bax-stable H9c2 cell line for apoptosis analysis. Am J Physiol Heart Circ Physiol 289:H477–H487
23. Sun B, Sun GB, Xiao J (2012) Isorhamnetin inhibits H (2) O (2)-induced activation of the intrinsic apoptotic pathway in H9c2 cardiomyocytes through scavenging reactive oxygen species and ERK inactivation. J Cell Biochem 113:473–485
24. Fröhlich GM, Meier P, White SK, Yellon DM, Hausenloy DJ (2013) Myocardial reperfusion injury: looking beyond primary PCI. Eur Heart J 34:1714–1722
25. Li R, Yan G, Li Q (2012) MicroRNA-145 protects cardiomyocytes against hydrogen peroxide (H_2O_2)-induced apoptosis through targeting the mitochondria apoptotic pathway. PLoS One 7:e44907
26. Crow MT, Mani K, Nam YJ (2004) the mitochondrial death pathway and cardiac myocyte apoptosis. Circ Res 95:957–970
27. Shibuya M (2013) Vascular endothelial growth factor and its receptor system: physiological functions in angiogenesis and pathological roles in various diseases. J Biochem 153:13–19
28. Gerber HP, McMurtrey A, Kowalski J, Yan M, Keyt BA, Dixit V, Ferrara N (1998) Vascular endothelial growth factor regulates endothelial cell survival through the phosphatidylinositol 3′-kinase/Akt signal transduction pathway. Requirement for Flk-1/KDR activation. J Biol Chem 273:30336–30343
29. Fujio Y, Nguyen T, Wencker D (2000) Akt promotes survival of cardiomyocytes in vitro and protects against ischemia–reperfusion injury in mouse heart. Circulation 101:660–667
30. Fujio Y, Walsh K (1999) Akt mediates cytoprotection of endothelial cells by vascular endothelial growth factor in an anchorage-dependent manner. J Biol Chem 274:16349–16354
31. Jiang X, Wang X (2004) Cytochrome C-mediated apoptosis. Annu Rev Biochem 73:87–106
32. Zhao T, Zhao W, Meng W, Liu C, Chen Y, Gerling IC, Weber KT, Bhattacharya SK, Kumar R, Sun Y (2015) VEGF-C/VEGFR-3 pathway promotes myocyte hypertrophy and survival in the infarcted myocardium. Am J Transl Res 7:697–709
33. van Wamel AJ, Ruwhof C, van der Valk-Kokshoom LE, Schrier PI, van der Laarse A (2001) The role of angiotensin II, endothelin-1 and transforming growth factor-beta as autocrine/paracrine mediators of stretch-induced cardiomyocyte hypertrophy. Mol Cell Biochem 218:113–124
34. Taimeh Z, Loughran J, Birks EJ, Bolli R (2013) Vascular endothelial growth factor in heart failure. Nat Rev Cardiol 10:519–530